2,5-Diformylbenzene-1,4-diol: A Versatile Building Block for the Synthesis of Ditopic Redox-Active Schiff Base Ligands

Tonia Kretz, Jan Willem Bats, Hans-Wolfram Lerner, and Matthias Wagner

Institut für Anorganische Chemie, Johann Wolfgang Goethe-Universität Frankfurt am Main, Max-von-Laue-Straße 7, 60438 Frankfurt am Main, Germany

Reprint requests to Prof. Dr. Matthias Wagner. Fax: +49 69 798 29260.
E-mail: Matthias.Wagner@chemie.uni-frankfurt.de

Z. Naturforsch. **2007**, *62b*, 66 – 74; received July 24, 2006

2,5-Diformylbenzene-1,4-diol (**5**) is a well-suited starting compound for the preparation of ditopic hydroquinone-based ligands. Here, we report an optimized synthesis of **5** which improves the overall yield from published 7 % to 42 %. Three new ditopic Schiff base ligands, 2,5-[^{i}Pr$_2$N(CH$_2$)$_2$N=CH]$_2$-1,4-(OH)$_2$-C$_6$H$_2$ (**8**), 2,5-(pyCH$_2$N=CH)$_2$-1,4-(OH)$_2$-C$_6$H$_2$ (**9**), and 2,5-[py(CH$_2$)$_2$N=CH]$_2$-1,4-(OH)$_2$-C$_6$H$_2$ (**10**), have been synthesized from **5** and structurally characterized by X-ray crystal structure analysis (py = 2-pyridyl).

Key words: Aldehydes, N,O Ligands, π-Interactions, Quinones, Tridentate Ligands

Introduction

The electrochemical properties of a metal complex are to a large extent determined by the ligand sphere. Careful ligand design is therefore crucial for the construction of efficient redox systems which in turn play an essential role both in homogeneous catalysis and in materials science [1 – 4].

Our group is interested in the electrochemical properties of oligonuclear transition metal complexes with electronically interacting metal sites. We thus require ligands capable of linking two or more transition metal centers and of supporting an electronic communication between them [5 – 7]. The concept is to modulate the degree of metal-metal interactions by electrochemical manipulation of the bridging unit which thus needs to be able to undergo reversible electron transfer itself. Currently, one focus lies on hydroquinone derivatives as bridging ligands since they exist in three different oxidation states (hydroquinone, semiquinone, quinone) and their redox-activity is preserved after metal coordination. In the literature, only very few chelating ditopic ligands derived from hydroquinone have been reported [8 – 11]. One example is the compound 2,5-bis(pyrazol-1-yl)-1,4-dihydroxybenzene [8] which we have used for the synthesis and structural characterization of the Cu^{II}-containing coordination polymer **A** (Fig. 1) [11, 12]. For an understanding of its electronic properties it was also necessary to synthesize dinuclear complexes **B** as soluble model systems (Fig. 1). However, attempts to prepare **B**-type molecules by treating 2,5-bis(pyrazol-1-yl)-1,4-dihydroxy-benzene with appropriate Cu^{II}-containing precursors in the presence of Brønsted bases were hampered by the pronounced tendency of the system to form polymers **A**. The only dinuclear complex **B** that could be isolated so far required PMDTA as an ancillary ligand and proved to be unstable in solution [11].

Due to this fact we had to develop an alternative hydroquinone linker and have chosen chelating Schiff base ligands **C** as our target molecules (Fig. 1). In

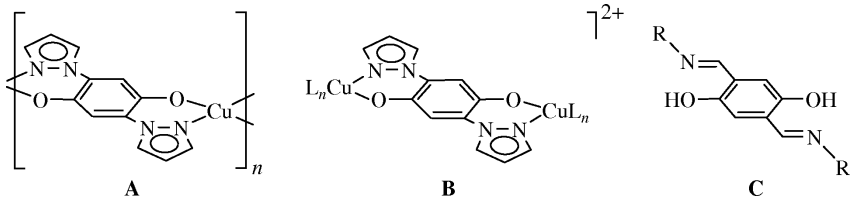

Fig. 1. The Cu^{II} coordination polymer **A** based on the 2,5-bis(pyrazol-1-yl)-1,4-dihydroxy-benzene ligand, the corresponding dinuclear complexes **B**, and the new ditopic hydroquinone Schiff base ligands **C**.

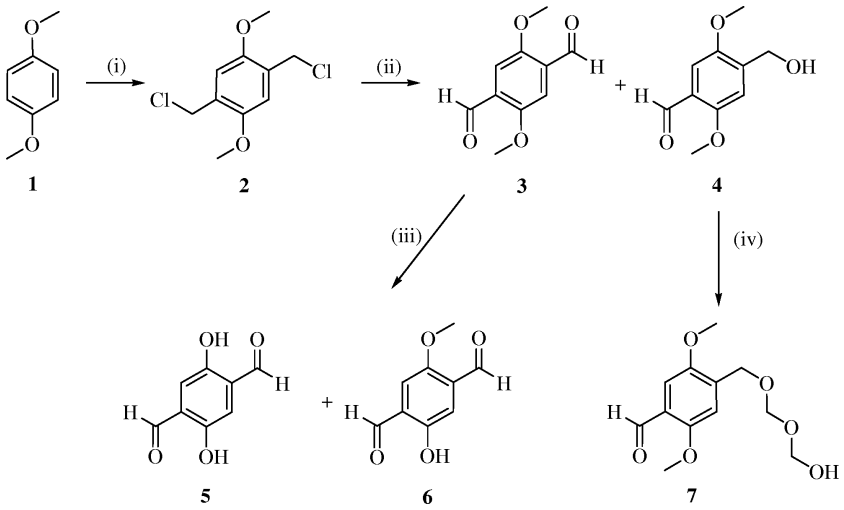

Scheme 1. Synthesis of **5**: (i) CH_2O_{aq}, HCl (yield: 86 %); (ii) 1. hexamethylenetetramine, 2. H_2O, HCl (yield: 70 %); (iii) HBr_{aq}, CH_3COOH (yield: 69 %); (iv) CH_2O_{aq}.

order to give the resulting dinuclear complexes more stability, we incorporated additional donor sites into the imine side-chains R. For the synthesis of **C**, the 2,5-diformylbenzene-1,4-diol (**5**) is required as the key starting material. Compound **5** (Scheme 1) is already known but was obtained in an overall yield of only 7 % to 20 % [13 – 15]. Moreover, none of the reaction byproducts were identified. The purpose of this paper is to report an improved synthesis of **5** together with a full characterization of the main reaction intermediates as well as some byproducts. Finally, the syntheses and molecular structures of selected **C**-type ligands are described.

Results and Discussion

Syntheses

The synthesis of **5** starts with the chloromethylation of commercially available 1,4-dimethoxy-benzene (**1**) to give the *p*-bis(chloromethyl)-benzene **2** (Scheme 1). Compared to the published protocol [13] the yield of **2** was improved from 77 % to 86 % by running the reaction at 0 °C as opposed to r. t., and by shortening the reaction time from 3 h to 1 h.

In the subsequent step, **2** was subjected to a Sommelet reaction to afford the dialdehyde **3** [14]. To find a way to improve the low reported yield [14] of **3** (32 %), the nature of the byproducts was determined by NMR spectroscopy. In addition to the resonances of the desired dialdehyde, the proton spectrum of the crude reaction mixture showed a signal at $\delta = 4.69$ assignable to the RC*H*$_2$OH fragment of an aliphatic alcohol. In the methoxy region of the spectrum, two signals at 3.87 and 3.80 ppm (integral ratio 1 : 1) indicated the presence of an unsymmetrically substituted 1,4-dimethoxy-benzene derivative. After isolation by flash chromatography and structural characterization by X-ray crystallography, the byproduct was identified as compound **4**. The formation of **4** can be explained after a closer look at the mechanism of the Sommelet reaction: addition of hexamethylenetetramine to an organochloride RCH_2Cl leads to the formation of a quaternary ammonium salt $[RCH_2N(CH_2)_6N_3]Cl$ which upon hydrolysis liberates formaldehyde and ammonia. The resulting primary amine RCH_2NH_2 is then oxidized to the imine which reacts further to the desired aldehyde RC(O)H. There are three possibilities for an alcohol RCH_2OH to be formed during this reaction sequence: 1) hydrolysis of residual RCH_2Cl that has not been transformed into the ammonium salt, 2) nucleophilic substitution of $C_6H_{12}N_4$ by water in the ammonium salt, and 3) a crossed Cannizzaro reaction [16, 17] between RC(O)H and formaldehyde. Alcohol **4** may even react further with formaldehyde to give acetal **7** as indicated by the ^{1}H NMR spectrum and the mass spectrum of the crude reaction mixture. The formation of **7** was verified in an independent experiment where we added an analytically pure sample of **4** to aqueous formaldehyde. The reaction is reversible since compound **4** was fully recovered after treatment of **7** with hydrochloric acid. Following the procedure described in the Experimental Section of this paper, we have reproducibly obtained **3** in a yield of 70 % rather than 32 % [14]. Phenolether **3**

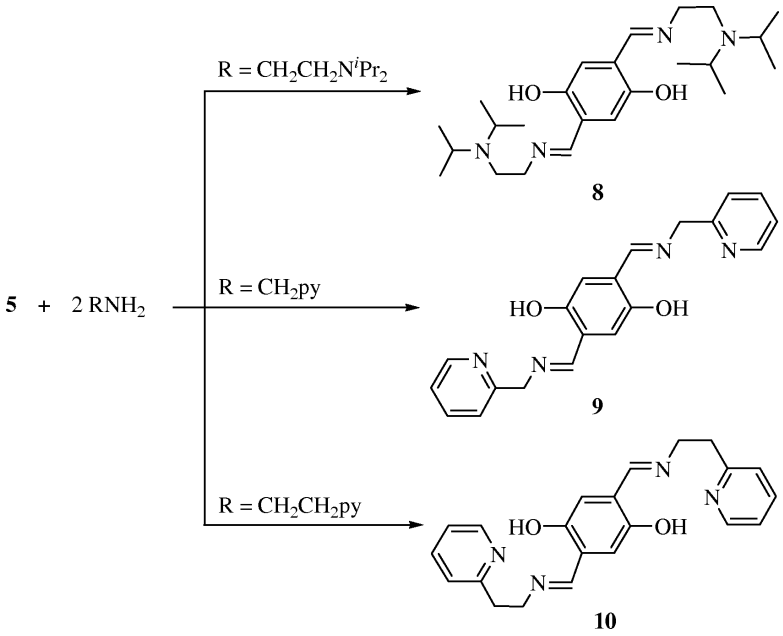

Scheme 2. Synthesis of the Schiff base ligands **8** – **10**.

was deprotected to give hydroquinone **5** using hydrobromic and acetic acid. After the recommended [15] reaction time of 5 h, a mixture of the desired compound **5** and the monomethylated dialdehyde **6** was obtained. Flash chromatography gave **5** in the reported yield of 30 % [15]. The yield of **5** could be improved to 69 % by extending the reaction time and continuous monitoring of the reaction progress by thin-layer chromatography (TLC).

The Schiff bases **8**, **9**, and **10** were prepared by treating 1 equiv. of **5** with 2 equiv. of 2-(diisopropylamino) ethylamine (**8**), 2-(aminomethyl)pyridine (**9**), or 2-(2-aminoethyl)pyridine (**10**; Scheme 2) [18]. These amines were chosen such that ligands of differing steric demand (*i. e.* **8** and **9**) and different length of the chelating tether (*i. e.* **9** and **10**) are now available for complexation studies.

NMR spectroscopic investigations

The ^{1}H NMR spectrum of **2** is characterized by a signal at 4.64 ppm assignable to the chloromethyl groups ($\delta(^{13}\mathrm{C}) = 41.3$). The successful synthesis of **3** by the Sommelet reaction is proven by the presence of aldehyde resonances at $\delta(^1\mathrm{H}) = 10.50$ and $\delta(^{13}\mathrm{C}) = 189.2$. In the NMR spectra of **5**, methoxy signals are absent and a broad proton resonance at 10.74 ppm (s, 2 H) appears instead, testifying to the presence of two free hydroxyl groups. For all three Schiff base ligands **8** – **10**, resonance patterns in accord with the postulated molecular symmetry are observed. Moreover, an integral ratio of 2 : 1 for the proton resonances of the imine substituents as compared to the signals of the central hydroquinone core indicates the quantitative transformation of aldehyde groups into imino side chains. All ^{1}H and ^{13}C NMR signals of **8** – **10** appear in the expected regions of the spectra and thus do not merit further discussion.

X-Ray crystal structure analyses

Details of the X-ray crystal structure analyses of **2** – **4**, **6**, and **8** – **10** are summarized in Table 1. The molecular structures are shown in Figs 2 – 8; selected bond lengths and angles are listed in the corresponding figure captions.

In the crystal lattice, the planar molecules **2**, **3**, **4**, and **6** are arranged in stacks *via* intermolecular $\pi\cdots\pi$-interactions. Adjacent stacks are linked *via* hydrogen bonds. All bond lengths and angles possess typical values for this type of compounds.

The chloromethylated hydroquinone derivative **2** (Fig. 2) is centrosymmetric, with half a molecule in the asymmetric unit, and crystallizes in the triclinic space group $P\bar{1}$. There are no short intramolecular interactions. The shortest intermolecular C$\cdots$C π-contact between molecules of the same stack amounts to 3.419(1) Å. Neighboring stacks are con-

Table 1. Details of the X-ray crystal structure analyses of **2** – **4**, **6**, and **8** – **10**.

	2	**3**	**4**	**6**	**8**	**9**	**10**
Formula	$C_{10}H_{12}Cl_2O_2$	$C_{10}H_{10}O_4$	$C_{10}H_{12}O_4 \cdot 0.5CH_2Cl_2$	$C_9H_8O_4$	$C_{24}H_{42}N_4O_2$	$C_{20}H_{18}N_4O_2$	$C_{22}H_{22}N_4O_2$
f.w.	235.10	194.18	238.66	180.15	418.62	346.38	374.44
Color, shape	colorless, rod	yellow, rod	colorless, rod	yellow, rod	yellow, block	yellow, rod	yellow, block
Temp. (K)	149(2)	147(2)	147(2)	160(2)	153(2)	148(2)	154(2)
Crystal system	triclinic	triclinic	monoclinic	monoclinic	monoclinic	monoclinic	monoclinic
Space group	*P*1	*P*1	*C*2/*c*	$P2_1/n$	$P2_1/c$	$P2_1/c$	$P2_1/n$
a (Å)	4.3808(5)	7.1551(8)	20.988(2)	7.8265(19)	6.7012(15)	18.345(2)	6.1039(12)
b (Å)	7.8173(12)	8.0143(9)	4.5966(3)	7.3929(13)	9.5338(18)	3.8965(5)	4.6544(7)
c (Å)	8.0979(10)	8.4624(10)	23.0443(19)	14.547(3)	20.052(3)	11.4271(15)	33.142(6)
α (deg)	90.454(9)	99.624(6)	90	90	90	90	90
β (deg)	91.235(7)	112.642(5)	95.491(5)	103.688(18)	98.926(16)	92.445(6)	93.037(14)
γ (deg)	105.072(7)	93.156(5)	90	90	90	90	90
V (Å^3)	267.69(6)	437.74(9)	2212.9(3)	817.8(3)	1265.6(4)	816.08(17)	940.2(3)
Z	1	2	8	4	2	2	2
$D_{calcd.}$ (g cm^{-3})	1.458	1.473	1.433	1.463	1.099	1.410	1.323
F(000)	122	204	1000	376	460	364	396
μ (mm^{-1})	0.577	0.115	0.339	0.117	0.070	0.094	0.087
Cryst. size (mm)	$0.90 \times 0.18 \times 0.10$	$0.50 \times 0.11 \times 0.07$	$0.60 \times 0.25 \times 0.08$	$0.56 \times 0.28 \times 0.15$	$0.26 \times 0.26 \times 0.26$	$0.90 \times 0.18 \times 0.03$	$0.20 \times 0.14 \times 0.12$
Reflections collected	4708	5988	18689	10412	13904	9248	6354
Indep. reflns. (R_{int})	1679 (0.036)	2614 (0.0264)	3666, 0.0324	2607, 0.0208	3147, 0.0607	2279, 0.0663	2085, 0.0802
Data/restraints/params.	1679 / 0 / 88	2614 / 0 / 167	3666 / 0 / 193	2607 / 0 / 151	3147 / 0 / 145	2279 / 0 / 154	2085 / 0 / 128
GOOF on F^2	1.06	1.07	1.05	1.05	1.098	0.91	1.12
*R*1, *wR*2($I \geq 2\sigma(I)$)	0.028, 0.075	0.044, 0.109	0.036, 0.084	0.035, 0.096	0.078, 0.122	0.051, 0.092	0.074, 0.112
*R*1, *wR*2 (all data)	0.032, 0.078	0.071, 0.125	0.058, 0.093	0.051, 0.101	0.142, 0.140	0.116, 0.107	0.158, 0.139
Largest diff. peak and hole (eÅ^{-3})	0.46 and −0.28	0.36 and −0.28	0.38 and −0.32	0.35 and −0.22	0.20 and −0.17	0.28 and −0.19	0.24 and −0.27

Fig. 2. Molecular structure of **2** in the solid state; thermal ellipsoids are drawn at the 50 % probability level. Selected bond lengths (Å), bond angles (deg), and torsion angles (deg): C(3)–C(5) 1.493(1), C(5)–Cl 1.821(1), C(2)–O 1.368(1), C(4)–O 1.430(1); C(3)–C(5)–Cl 110.9(1), C(2)–O–C(4) 117.2(1); C(1)–C(2)–O–C(4) −0.7(1), C(2)–C(3)–C(5)–Cl −77.9(1). Symmetry transformations used to generate equivalent atoms: #1 $-x, -y+1, -z+1$.

Fig. 3. Molecular structure of **3** in the solid state; thermal ellipsoids are drawn at the 50 % probability level. Selected bond lengths (Å), bond angles (deg), and torsion angles (deg) of molecule 1: C(2)–C(5) 1.480(2), C(1)–O(1) 1.366(1), C(4)–O(1) 1.438(1), C(5)–O(2) 1.208(2); C(1)–O(1)–C(4) 117.2(1), C(2)–C(5)–O(2) 123.6(1); C(1)–C(2)–C(5)–O(2) −174.4(1), C(2)–C(1)–O(1)–C(4) −177.8(1). Symmetry transformations used to generate equivalent atoms: #1 $-x, -y, -z$; #2 $-x+1, -y+2, -z$.

nected by C–H···Cl and C–H···O hydrogen bonds with H···Cl distances of 2.90(2) and 3.02(2) Å, respectively, and an H···O distance of 2.60(2) Å.

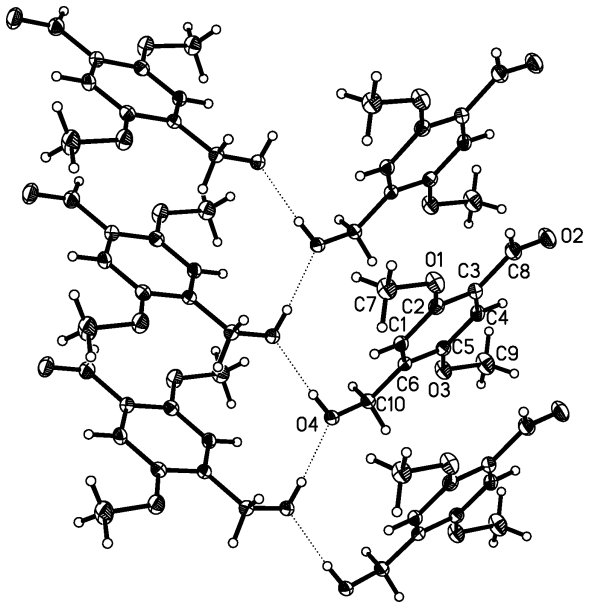

Fig. 4. Molecular structure of **4** in the solid state; thermal ellipsoids are drawn at the 50 % probability level. Selected bond lengths (Å), bond angles (deg), and torsion angles (deg): C(3)–C(8) 1.473(2), C(6)–C(10) 1.510(1), C(2)–O(1) 1.368(1), C(5)–O(3) 1.373(1), C(8)–O(2) 1.218(1), C(10)–O(4) 1.425(1); C(2)–O(1)–C(7) 117.1(1), C(3)–C(8)–O(2) 123.7(1), C(5)–O(3)–C(9) 116.2(1), C(6)–C(10)–O(4) 113.1(1); C(1)–C(2)–O(1)–C(7) −14.2(2), C(2)–C(3)–C(8)–O(2) 178.3(1), C(4)–C(5)–O(3)–C(9) 13.3(2), C(1)–C(6)–C(10)–O(4) −5.0(1). Symmetry transformations used to generate equivalent atoms: $^{\#1}$ $-x$, y, $-z+1/2$.

Fig. 3 illustrates the structure of dialdehyde **3** in the solid state (triclinic space group $P\bar{1}$). Each of the two independent molecules is centrosymmetric, two half molecules thus being present in the asymmetric unit. Since their structural parameters do not differ significantly from each other, only the values of molecule 1 are given here. The methoxy as well as the aldehyde groups are almost coplanar with the phenyl rings (deviation of C(4)/O(2) from the plane of the phenylene ring: 0.033/0.088 Å). There is a short intramolecular interaction between the aldehyde hydrogen atom and its neighboring methoxy oxygen atom of H(5)···O(1) = 2.40(2) Å with a bond angle C(5)–H(5)···O(1) of 101(1)°. The shortest C···C contact between molecules of the same stack is 3.293(2) Å. Stacks are linked *via* intermolecular C–H···O contacts between aldehyde oxygen atoms and methoxy methyl groups (H···O = 2.53(2) to 2.63(2) Å).

The byproduct **4** crystallizes from CH_2Cl_2 (monoclinic space group $C2/c$, Fig. 4). There are one molecule of **4** and half a solvent molecule in the asymmetric unit. The X-ray crystal structure analysis fully confirms our interpretation of the NMR spectra in that **4** contains an aldehyde group together with a hydroxymethyl substituent. The stacks of **4** have short C···C distances in the range between 3.426(1) to 3.546(1) Å. Adjacent stacks are connected by intermolecular hydrogen bonds between hydroxymethyl groups (H···O = 1.90(2) Å, angle O-H-O = 175(2)°).

The molecular structure of the partly deprotected byproduct **6** (monoclinic, $P2_1/n$) is plotted in Fig. 5. All side groups are nearly coplanar with the central six-membered ring (C(2)–C(3)–C(7)–O(2) = 0.8(2)°, C(4)-C(5)-O(3)-C(8) = 1.7(1)°, C(1)–C(6)–C(9)–O(4) = −3.1(1)°). Each hydroxyl group establishes a bifurcated hydrogen bond to two aldehyde oxygen atoms (intramolecular: H···O = 1.92(2) Å; intermolecular: H···O = 2.29(2) Å).

In the three Schiff bases **8**, **9**, and **10** (Figures 6–8), the C(4)–N(1) bond lengths vary in the small range between 1.273(2) (**8**) and 1.278(3) Å (**10**) which is characteristic of imine double bonds. These C=N fragments as well as the hydroxyl groups are largely coplanar with the respective central six-membered ring and linked by intramolecular hydrogen bonds (OH···N distances vary from 1.77(3) to 1.90(2) Å).

Fig. 6 shows the molecular structure of **8** (monoclinic space group $P2_1/c$). Because of the bulky 2-(diisopropylamino)ethyl substituents at the imino nitrogen atoms, **8** is the only compound which is not arranged in stacks in the solid state. The conformation of the diisoproylamino groups can be regarded as intermediate between planar and pyramidal (sum of the three valence angles about N(2) = 345.7°).

Compound **9** also crystallizes in the monoclinic space group $P2_1/c$ (Fig. 7). Each pyridyl ring includes a dihedral angle of 46.7° with the aromatic bridge. The crystal lattice consists of columns of molecules along the crystallographic *b* axis. Molecules within each stack show intermolecular C···C distances of 3.387(2) Å between phenyl groups and of 3.560(3) Å between pyridyl groups.

In the solid state, **10** (monoclinic, $P2_1/n$; Fig. 8) also features stacks of molecules along the crystallographic *b* axis. In contrast to **9**, the pyridyl rings in **10** are almost coplanar with the aromatic linker (dihedral angle = 6.7°).

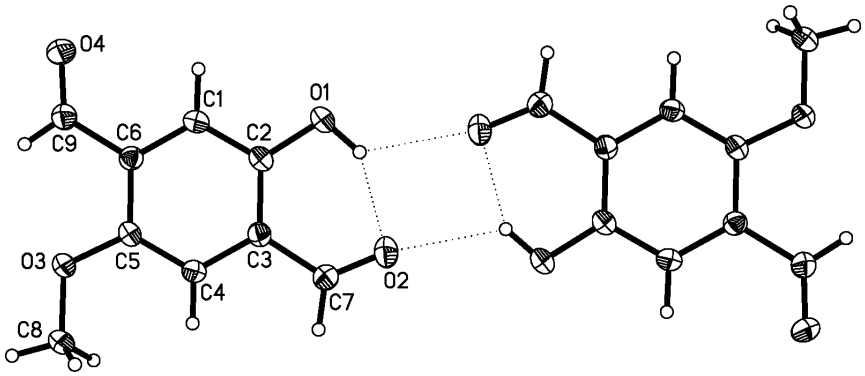

Fig. 5. Molecular structure of **6** in the solid state; thermal ellipsoids are drawn at the 50 % probability level. Selected bond lengths (Å), bond angles (deg), and torsion angles (deg): C(3)–C(7) 1.464(1), C(6)–C(9) 1.478(1), C(2)–O(1) 1.356(1), C(5)–O(3) 1.364(1), C(7)–O(2) 1.216(1), C(9)–O(4) 1.212(1); C(3)–C(7)–O(2) 124.3(1), C(5)–O(3)–C(8) 116.9(1), C(6)–C(9)–O(4) 123.6(1); C(2)–C(3)–C(7)–O(2) 0.8(2), C(4)–C(5)–O(3)–C(8) 1.7(1), C(1)–C(6)–C(9)–O(4) −3.1(1).

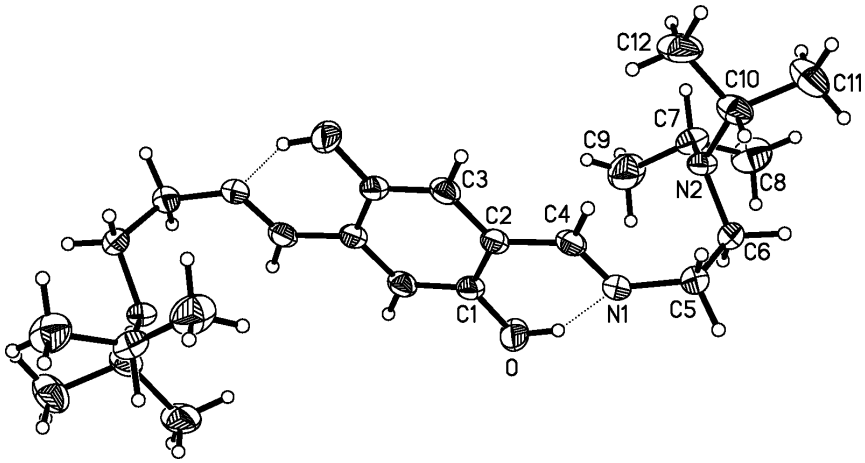

Fig. 6. Molecular structure of **8** in the solid state; thermal ellipsoids are drawn at the 50 % probability level. Selected bond lengths (Å), bond angles (deg), and torsion angles (deg): C(1)–O 1.361(2), C(2)–C(4) 1.456(3), C(4)–N(1) 1.273(2), C(5)–N(1) 1.457(3), C(6)–N(2) 1.459(2); C(2)–C(4)–N(1) 122.3(2), C(4)–N(1)–C(5) 117.6(2), C(6)–N(2)–C(7) 115.0(2), C(6)–N(2)–C(10) 113.8(2), C(7)–N(2)–C(10) 116.9(2); C(3)–C(2)–C(4)–N(1) 179.8(2), C(4)–N(1)–C(5)–C(6) −96.9(2), N(1)–C(5)–C(6)–N(2) 62.7(2). Symmetry transformations used to generate equivalent atoms: $^{\#1}$ $-x, -y+1, -z$.

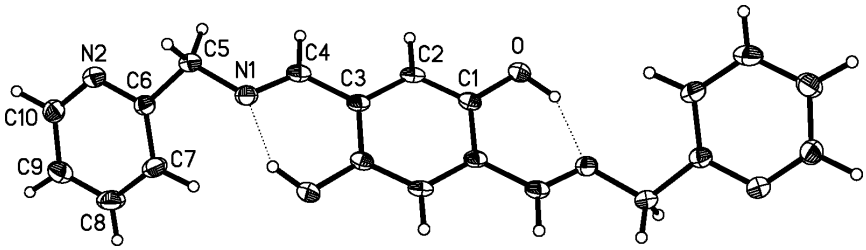

Fig. 7. Molecular structure of **9** in the solid state; thermal ellipsoids are drawn at the 50 % probability level. Selected bond lengths (Å), bond angles (deg), and torsion angles (deg): C(1)–O 1.364(2), C(3)–C(4) 1.465(2), C(4)–N(1) 1.275(2), C(5)–N(1) 1.459(2); C(3)–C(4)–N(1) 122.0(2), C(4)–N(1)–C(5) 117.6(1); C(2)–C(3)–C(4)–N(1) −176.9(2), C(3)–C(4)–N(1)–C(5) −179.1(1), C(4)–N(1)–C(5)–C(6) 129.1(2). Symmetry transformations used to generate equivalent atoms: $^{\#1}$ $-x, -y+1, -z+2$.

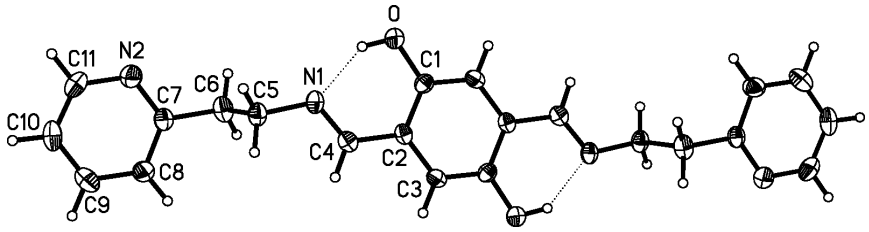

Fig. 8. Molecular structure of **10** in the solid state; C(1)–O 1.365(3), C(2)–C(4) 1.460(4), C(4)–N(1) 1.278(3), C(5)–N(1) 1.466(3); C(2)–C(4)–N(1) 122.3(3), C(4)–N(1)–C(5) 117.7(2); C(1)–C(2)–C(4)–N(1) 1.0(4), C(2)–C(4)–N(1)–C(5) 177.3(2), C(4)–N(1)–C(5)–C(6) −103.9(3), N(1)–C(5)–C(6)–C(7) −177.9(2). Symmetry transformations used to generate equivalent atoms: $^{\#1}$ $-x+2, -y+3, -z$.

Conclusion

The synthesis of 2,5-diformylbenzene-1,4-diol (**5**) has been improved from an overall yield of 7.4 to 41.5 %. As unwanted side reactions, we identified the reduction of aldehyde substituents to hydroxymethyl groups (*cf.* compound **4**) and a non-quantitative deprotection of the hydroquinone core in the last step of the synthesis sequence. Both side reactions could be suppressed to a considerable extent.

With this efficient synthesis of **5**, a variety of ditopic Schiff base ligands featuring a redox-active hydroquinone core are now readily available which are promising bridging ligands for the preparation of dinuclear transition metal complexes.

Experimental Section

General remarks

^{1}H and ^{13}C NMR spectra: Bruker AM 250, Bruker DPX 250 spectrometers. Chemical shift values (δ) are reported relative to tetramethylsilane; abbreviations: s (singlet), d (doublet), t (triplet), vt (virtual triplet), sept (septet), m (multiplet), py (2-pyridyl). ESI mass spectra: Fisons (now Micromass) VG Platform II. MALDI-TOF spectra: Fisons (now Micromass) VG Tofspec. Elemental analyses were performed by the microanalytical laboratory of the University of Frankfurt. Flash column chromatography: Merck silica gel 60 (40 – 60 μm, 230 – 400 mesh). Thin-layer chromatography (TLC): Merck silica plates (Kieselgel 60 F254 on aluminium with fluorescence indicator); spots on TLC plates were visualized by UV-detection at 254 nm. Solvents and reagents were purchased from Aldrich Chemicals, Merck and Fluka. $CHCl_3$ was dried over molecular sieves (4 Å).

*Synthesis of **2***

To a solution of 1,4-dimethoxybenzene (69.35 g, 0.50 mol) in dioxane (400 mL) and aqueous hydrochloric acid (37 %, 65 mL), three equal portions of aqueous formaldehyde (37 %; overall amount: 100.5 mL, 1.35 mol) were added at intervals of 30 min with stirring at 0 °C. During the entire period, hydrogen chloride gas was passed through the reaction mixture. After stirring for 1 h at r. t., more aqueous hydrochloric acid (37 %, 195 mL) was added and the resulting solution cooled to 10 °C. The colorless precipitate formed was collected on a frit and dried under vacuum. Recrystallization of **2** from acetone afforded X-ray quality crystals. Yield: 101.33 g (86 %). – ^{1}H NMR (250.13 MHz, $CDCl_3$): δ = 6.93 (s, 2 H, CH), 4.64 (s, 4 H, CH_2), 3.86 (s, 6 H, CH_3). – ^{13}C NMR (62.9 MHz, $CDCl_3$): δ = 151.1 (*C*OCH_3), 126.9 (*C*CH_2Cl), 113.4 (CH), 56.3 (CH_3), 41.3 (CH_2). – ESI-MS: m/z (%) = 199 (100) $[M\text{-}Cl]^+$. – $C_{10}H_{12}Cl_2O_2$ (235.1): calcd. C 51.09, H 5.14; found C 50.81, H 5.14.

*Synthesis of **3***

2 (10.00 g, 0.04 mol) and hexamethylenetetramine (11.2 g, 0.08 mol) were dissolved in anhydrous chloroform (150 mL) and the mixture heated to reflux for 3 h. Subsequent cooling to 5 °C led to the formation of a yellow microcrystalline solid which was isolated by filtration and redissolved in water (130 mL). The solution was heated to reflux for 2 h. After cooling to r. t., aqueous hydrochloric acid (37 %, 5 mL) was added, whereupon a yellow solid precipitated from the solution. This crude product was collected on a frit. The aqueous filtrate was extracted with chloroform (5 × 30 mL), the extracts were dried over magnesium sulfate, filtered, and evaporated to dryness under reduced pressure to yield a second crop of product. Subsequent flash chromatography (dichloromethane/ethyl acetate, 2 : 1) provided **3** and **4** as yellow solids. Recrystallization of **3** from dichloromethane/hexane (1 : 1) afforded X-ray quality crystals. Yield of **3**: 5.40 g (70 %).

*Analytical data of **3**: R_f* (dichloromethane/ethyl acetate, 2 : 1) = 0.87. – ^{1}H NMR (250.13 MHz, $CDCl_3$): δ = 10.50 (s, 2 H, CHO), 7.45 (s, 2 H, CH), 3.94 (s, 6 H, CH_3). – ^{13}C NMR (62.9 MHz, $CDCl_3$): δ = 189.2 (CHO), 155.7 (*C*OCH_3), 129.1 (*C*CHO), 110.9 (CH), 56.2 (CH_3). – ESI-MS: m/z (%) = 194 (100) $[M]^+$. – $C_{10}H_{10}O_4$ (194.2): calcd. C 61.85, H 5.19; found C 61.61, H 5.24.

*Analytical data of **4**:* R_f (dichloromethane/ethyl acetate, 2 : 1) = 0.45. – ^{1}H NMR (250.13 MHz, $CDCl_3$): δ = 10.38 (s, 1 H, CHO), 7.24, 7.04 (2× s, 2 × 1 H, CH), 4.69 (s, 2 H, CH_2), 3.87, 3.80 (2× s, 2 × 3 H, CH_3) 2.53 (s, 1H, OH). – ^{13}C NMR (62.9 MHz, $CDCl_3$): δ = 189.3 (CHO), 156.9, 150.8 (*C*OCH_3), 138.1 (*C*CH_2OH), 123.6 (*C*CHO), 111.8, 107.9 (CH), 61.2 (CH_2), 56.2, 55.7 (CH_3). – ESI-MS: m/z (%) = 196 (100) $[M]^+$. – $C_{10}H_{12}O_4 \cdot 0.33\ H_2O$ (202.1): calcd. C 59.40, H 6.31; found C 59.13, H 6.34.

*Synthesis of **5***

A mixture of **3** (3.71 g, 0.02 mol), acetic acid (99.5 %, 190 mL) and aqueous hydrobromic acid (48 %, 160 mL) was heated to reflux for 14 h. After cooling to r. t., the solution was poured into a mixture of chloroform and water (150 mL, 1 : 1), the aqueous layer was extracted with chloroform (3 × 75 mL) and the combined organic phases were dried over magnesium sulfate. After filtration, the filtrate was evaporated to dryness under reduced pressure to give **5** as a yellow solid. Yield: 2.31 g (69 %). – R_f (ethyl acetate/hexane, 1 : 1) = 0.47. – ^{1}H NMR (250.13 MHz, DMF): δ = 10.74 (s, 2 H, OH), 10.42 (s, 2 H, CHO), 7.36 (s, 2 H, CH). – ^{13}C NMR (62.9 MHz, DMF): δ = 191.8 (CHO), 153.8 (COH), 128.2 (*C*CHO), 116.6 (CH). – ESI-MS: m/z (%) = 165 (100) $[M\text{-}H]^-$. – $C_8H_6O_4 \cdot 0.25\ H_2O$ (170.6): calcd. C 56.31, H 3.84; found C 56.66, H 3.77. Our optimised synthesis protocol does not lead to detectable amounts of **6**. In contrast, if the published [15] synthesis protocol is followed, substantial amounts of **6** are formed as byproduct. Compounds **5** and **6** can be separated by flash chromatography (ethyl acetate/hexane, 1 : 1).

*Analytical data of **6**:* R_f (ethyl acetate/hexane, 1 : 1) = 0.40. – ^{1}H NMR (250.13 MHz, DMF): δ =10.72 (s, 1 H, OH), 10.41 (s, 2 H, CHO), 7.46, 7.37 (2× s, 2 × 1 H, CH), 3.97 (s, 3 H, CH_3). – ^{13}C NMR (62.9 MHz, DMF): δ = 191.5, 189.4 (CHO), 155.1, 154.9 (COH, *C*OCH_3), 130.3, 127.4 (*C*CHO), 116.1, 112.1 (CH), 56.5 (CH_3).

*General procedure for the synthesis of **8**, **9**, and **10***

5 (162 mg, 1 mmol) and the appropriate amine (2 mmol) were dissolved in methylene chloride (70 mL) and the solution heated to reflux for 1 h. After cooling to r. t. all volatiles were evaporated under reduced pressure and the remaining crude product recrystallized from acetonitrile.

*Analytical data of **8**:* Yield: 376 mg (90 %), brown solid. – ^{1}H NMR (250.13 MHz, CD_2Cl_2): δ = 12.75 (s, 2 H, OH), 8.24 (s, 2 H, HC=N), 6.83 (s, 2 H, CH), 3.58 (t, ^3JHH = 6.4 Hz, 4 H, CH_2), 3.01 (sept, ^3JHH = 6.6 Hz, 4 H, C*H*$(CH_3)_2$), 2.75 (t, ^3JHH = 6.4 Hz, 4 H, CH_2), 0.98 (d, ^3JHH = 6.6 Hz, 24 H, CH_3). – ^{13}C NMR (62.9 MHz, CD_2Cl_2): δ = 164.9 (C=N), 152.8 (COH), 121.4 (*C*CHN), 117.9 (CH), 61.0 (CH_2), 48.6 (*C*H$(CH_3)_2$), 45.7 (CH_2), 20.7 (CH_3). – ESI-MS: m/z (%) = 419 (100) $[M+H]^+$. – $C_{24}H_{42}N_4O_2$ (418.6): calcd. C 68.86, H 10.11, N 13.38; found C 68.37, H 10.22, N 13.07.

*Analytical data of **9**:* Yield: 291 mg (84 %), orange solid. – ^{1}H NMR (250.13 MHz, CD_2Cl_2): δ = 12.48 (s, 2 H, OH), 8.56 (d, ^3JHH = 4.4 Hz, 2 H, py-H6), 8.51 (s, 2 H, HC=N), 7.71 (vt, ^3JHH = 7.7 Hz, 2 H, py-H4), 7.35 (d, ^3JHH = 7.9 Hz, 2 H, py-H3), 7.22 (vt, ^3JHH = 5.2 Hz, 2 H, py-H5), 6.93 (s, 2 H, CH), 4.94 (s, 4 H, CH_2). – ^{13}C NMR (62.9 MHz, CD_2Cl_2): δ = 166.4 (C=N), 157.9 (py-C2), 152.8 (COH), 149.6 (py-C6), 136.8 (py-C4), 122.4, 122.1, 121.7 (*C*CHN, py-C3,5), 118.5 (CH), 65.4 (CH_2). – MALDI-TOF-MS [positive ions, matrix: 6-aza-2-thiothymine (ATT)]: m/z = 346 $[M]^+$. – $C_{20}H_{18}N_4O_2$ (346.4): calcd. C 69.35, H 5.24, N 16.17; found C 69.19, H 5.26, N 16.07.

*Analytical data of **10**:* Yield: 333 mg (89 %), orange solid. – ^{1}H NMR (250.13 MHz, CD_2Cl_2): δ = 12.45 (s, 2 H, OH), 8.52 (d, ^3JHH = 5.0 Hz, 2 H, py-H6), 8.25 (s, 2 H, HC=N), 7.60 (vt, ^3JHH = 7.8 Hz, 2 H, py-H4), 7.15 (m, 4 H, py-H3,5), 6.75 (s, 2 H, CH), 4.02, 3.15 (2× t, ^3JHH = 7.1 Hz, 2 × 4 H, CH_2). – ^{13}C NMR (62.9 MHz, CD_2Cl_2): δ = 165.2 (C=N), 159.6 (py-C2), 152.9 (COH), 149.8 (py-C6), 136.5 (py-C4), 123.8 (py-C3 or 5), 121.7, 121.6 (*C*CHN, py-C3 or 5), 118.3 (CH), 59.6 (CH_2), 39.5 (CH_2py). – MALDI-TOF-MS [positive ions, matrix: 2,5-dihydroxybenzoic acid (DHB)]: m/z = 374 $[M]^+$. – $C_{22}H_{22}N_4O_2 \cdot 0.5\ H_2O$ (383.4): calcd. C 68.91, H 6.05, N 14.61; found C 68.57, H 5.92, N 14.60.

X-Ray crystal structure analyses

The single crystal X-ray measurements were performed on a Siemens SMART CCD diffractometer using monochromated Mo K_α radiation. Repeatedly measured standard reflections remained stable. Numerical absorption corrections were performed for **2** and **3**, empirical absorption corrections [20] were applied for **4**, **6**, **8**, and **9**. No absorption correction was made for **10**. The structures were determined by Direct Methods using SHELXS-97 [21] and refined on F^2 values using the program SHELXL-97 [21]. H-atoms were geometrically positioned and were constrained for **8** and **10**. H-atom positions were taken from a difference Fourier map and were refined for **2**, **3**, **4**, **6**, and **9**.

CCDC-608824 (**2**), CCDC-608825 (**3**), CCDC-608826 (**4**), CCDC-608827 (**6**), CCDC-608828 (**8**), CCDC-608829 (**9**) and CCDC-608830 (**10**) contain the supplementary crystallographic data for this paper. These data can be obtained free of charge from The Cambridge Crystallographic Data Centre *via* http://www.ccdc.cam.ac.uk/datarequest/cif.

Acknowledgements

This work was supported by the Deutsche Forschungsgemeinschaft and the Fonds der Chemischen Industrie.

[1] A. M. Allgeier, C. A. Mirkin, *Angew. Chem.* **1998**, *110*, 936; *Angew. Chem. Int. Ed.* **1998**, *37*, 894.
[2] E. Evangelio, D. Ruiz-Molina, *Eur. J. Inorg. Chem.* **2005**, 2957.
[3] T. Hirao, *Coord. Chem. Rev.* **2002**, *226*, 81.
[4] T. Moriuchi, T. Watanabe, I. Ikeda, A. Ogawa, T. Hirao, *Eur. J. Inorg. Chem.* **2001**, 277.
[5] A. Tárraga, P. Molina, D. Curiel, M. D. Velasco, *Organometallics* **2001**, *20*, 2145.
[6] J. A. McCleverty, M. D. Ward, *Acc. Chem. Res.* **1998**, *31*, 842.
[7] V. Lloveras, J. Vidal-Gancedo, D. Ruiz-Molina, T. M. Figueira-Duarte, J.-F. Nierengarten, J. Veciana, C. Rovira, *Faraday Discuss.* **2006**, *131*, 291.
[8] W. Gauß, H. Heitzer, S. Petersen, *Liebigs Ann. Chem.* **1972**, *764*, 131.
[9] C. Drouza, A. D. Keramidas, *J. Inorg. Biochem.* **2000**, *80*, 75.
[10] M. Kato, K. Nakajima, Y. Yoshikawa, M. Hirotsu, M. Kojima, *Inorg. Chim. Acta* **2000**, *311*, 69.
[11] G. Margraf, T. Kretz, F. Fabrizi de Biani, F. Laschi, S. Losi, P. Zanello, J. W. Bats, B. Wolf, K. Remović-Langer, M. Lang, A. Prokofiev, W. Aßmus, H.-W. Lerner, M. Wagner, *Inorg. Chem.* **2006**, *45*, 1277.
[12] R. Dinnebier, H.-W. Lerner, L. Ding, K. Shankland, W. I. F. David, P. W. Stephens, M. Wagner, *Z. Anorg. Allg. Chem.* **2002**, *628*, 310.
[13] J. H. Wood, R. E. Gibson, *J. Am. Chem. Soc.* **1949**, *71*, 393.
[14] S. J. Angyal, P. J. Morris, J. R. Tetaz, J. G. Wilson, *J. Chem. Soc.* **1950**, 2141.
[15] a) D. E. Burton, K. Clarke, G. W. Gray, *J. Chem. Soc.* **1965**, 438; b) C.-C. Zeng, J. Y. Becker, *J. Org. Chem.* **2004**, *69*, 1053.
[16] S. Cannizzaro, *Justus Liebigs Ann. Chem.* **1853**, 129.
[17] T. A. Geissman, *Org. React.* **1944**, *2*, 94.
[18] J. M. Mitchell, N. S. Finney, *J. Am. Chem. Soc.* **2001**, *123*, 862.
[19] T. Kretz, J. W. Bats, S. Losi, B. Wolf, H.-W. Lerner, M. Lang, P. Zanello, M. Wagner, *Dalton Trans.* **2006**, 4914.
[20] G. M. Sheldrick, SADABS, University of Göttingen (Germany) **2000**.
[21] a) G. M. Sheldrick, *Acta Crystallogr.* **1990**, *A46*, 467; b) G. M. Sheldrick, SHELXL-97. A Program for the Refinement of Crystal Structures, University of Göttingen (Germany) **1997**.